Physica E: Low-dimensional Systems and Nanostructures 114 (2019) 113647

Contents lists available at ScienceDirect

Physica E: Low-dimensional Systems and Nanostructures

journal homepage: www.elsevier.com/locate/physe

Intersubband optical properties of a laser-dressed asymmetric triple quantum well nanostructure

F. Ungan[a], M.E. Mora-Ramos[b], M.G. Barseghyan[c,*], L.M. Pérez[d], D. Laroze[d]

[a] Faculty of Technology, Department of Optical Engineering, Sivas Cumhuriyet University, 58140 Sivas, Turkey
[b] Centro de Investigación en Ciencias, Instituto de Investigación en Ciencias Básicas y Aplicadas, Universidad Autónoma del Estado de Morelos, Av. Universidad 1001, CP 62209, Cuernavaca, Morelos, Mexico
[c] Department of Solid State Physics, Yerevan State University, Alex Manoogian 1, 0025 Yerevan, Armenia
[d] Instituto de Alta Investigación, CEDENNA, Universidad de Tarapacá, Casilla 7D, Arica, Chile

ARTICLE INFO

Keywords:
δ-Doped quantum well
Intense laser field
Electric field
Magnetic field
Intersubband optical properties

ABSTRACT

The simultaneous effect of static electric and magnetic fields as well as the intense THz laser field on the intersubband nonlinear optical properties of n-type asymmetric triple δ-doped quantum well is theoretically investigated. The calculations are carried out within the framework of the effective-mass and parabolic-band approximations, with the use of a diagonalization technique to determine the electron energies and the wave functions. The analytical expression of the total absorption coefficient and the relative refractive change of the structure have been found by using the compact-density-matrix approach via an iterative method. The obtained results show that the strengthening of the electric and the magnetic fields, as well as the increment of laser field parameter, lead to a blue shift of the resonant peaks of the intersubband optical absorption and the relative refractive index change spectrum. Additionally, the strengthening of the external fields leads to the reinforcement of the total absorption spectrum intensity. Finally, we have found that with the decrease in the number of the well, by keeping the effective width of the structure constant, the blue shift can be observed in the total absorption spectrum. Therefore, the obtained results give an additional possibility to tune the performance of new devices, based on the quantum wells nanostructures.

1. Introduction

Due to the advances in modern semiconductor crystal growth and doping techniques, it has been possible to produce high quality δ-doped layers in low-dimensional semiconductor systems. These structures are formed via the compositional control on the layer growth thickness on a scale of several angstroms. Thanks to this technique, by changing the doping concentration, the confinement potential depth due to the conduction or valence band bending in the system can be adjusted according to the purpose. Compared to the bulk semiconductor materials, these structures show a discrete energy spectrum, and because of the strong quantum confinement effect, there is a small energy separation between the subband energy levels. Besides, the strong spatial overlap between confined states leads to large values of the electric dipole moment matrix elements. Since these features affect the electronic, optical, and transport properties of semiconductor systems, the delta-doping process can play an essential role in new device designs.

The single and multiple δ-doped quantum wells (QWs) are suitable systems not only for investigating the physics at extremely high donor concentrations but also for high power device applications [1–12]. The knowledge of the electronic states and optical properties related to the intersubband transitions in these systems is especially relevant for optoelectronic device design. It is well known that δ-doping is one of the processes of seeding a large amount of charge carriers in a semiconducting host material, looking for the generation of high conductivity strongly confined quasi-two-dimensional channels. This can lead to an improvement of the electronic operation of devices that incorporate this particular kind of doping, as the case of field effect transistors. The first proposal of a δ-doped device was put forward in Ref. [13] and consisted of a single δ-doped QW relatively close to a metal-semiconductor contact. This design is now referred to as a δ-doped field effect transistor.

The optical properties of semiconductor nanostructures such as oscillator strength, nonlinear optical rectification, total optical absorption coefficients, relative refractive index changes, second and third harmonic generations have been researched experimentally and theoretical

* Corresponding author.
E-mail address: mbarsegh@ysu.am (M.G. Barseghyan).

https://doi.org/10.1016/j.physe.2019.113647
Received 14 June 2019; Accepted 19 July 2019
Available online 19 July 2019
1386-9477/ © 2019 Elsevier B.V. All rights reserved.

by many authors [14–36]. The presented numerical results demonstrated that the optical properties of these systems are closely related to the presence of applied external fields, the structural parameters, the doping concentrations, and the shape and asymmetry of the confinement potential of the system. For example, Kim and co-authors [32] have analyzed the existence of high density two-dimensional electron gas. They defined the subband energy spectrum in the δ-doped GaAs/AlGaAs single QW by using the Shubnikov-de Haas and Van der Paw-Hall effect measurements at 1.5 K. The intersubband light absorption measurements on a series of GaAs/AlAs QWs with heavy delta-doping have been performed by Sasagawa et al. [33]. Yildirim and Tomak [34] theoretically studied the nonlinear intersubband optical absorption coefficients in delta-doped GaAs QW under the applied static electric field. Their numerical results demonstrate that the optical absorption coefficients are powerfully affected by the applied static electric field. Orozco and co-authors [35] theoretically analyzed the effect of the hydrostatic pressure on the nonlinear optical properties, in particular, nonlinear optical rectification, second harmonic generation, and third harmonic generation in GaAs δ-field-effect transistor structures. Almansour et al. [36] calculated the effect of the δ-doping on the subband structure and the nonlinear optical properties of InAlN/GaN single QWs. They found that the magnitude of the total optical absorption coefficients is strongly affected by the δ-doping concentrations. Recently, we have been investigated the effect of applied external fields on the total absorption coefficients and relative refractive index changes in a single, double, and triple δ-doped GaAs QWs in detail [37–40]. As summarized above, although several studies have been conducted on the optical features of δ-doped low-dimensional systems, to our knowledge no reports have focused on the effect of electric and magnetic fields on the total optical absorption coefficient and relative refractive index changes in an asymmetric triple δ-doped GaAs QWs under intense THz laser field (ILF). Therefore, this is the main motivation for this study and we aim to examine this subject in detail.

This article aims to analyze the effects of the electric and magnetic fields and high-frequency non-resonant ILF on the relative refractive index changes and total optical absorption coefficient in the asymmetric triple δ-doped GaAs QWs. The organization of the present study is as follows: In Section 2, we present the Hamiltonian of the asymmetric triple δ-doped GaAs QWs to calculate relevant subband energies and their wave functions. Then we give the analytical expression of the relative refractive index changes and total optical absorption coefficient obtained by the compact density matrix approach via the iterative method. In Sec. 3 the numerical results are shown and analyzed. Finally, the conclusions are given in Sec. 4.

2. Theoretical framework

As mentioned, the aim of this study is to research the influence of external perturbations, such as static electric, magnetic, and high-frequency intense laser fields on the electronic and optical properties of asymmetric triple δ-doped GaAs QW. In order to do this research, we assume that the high-frequency ILF polarization vector and the static electric field are directed along the growth direction of the system. Meanwhile, the static magnetic field is considered to be oriented perpendicular to the growth direction. Based on the effective mass and parabolic band approximations, the Hamiltonian of an electron confined in an asymmetric triple δ-doped GaAs QW under the impact of the above mentioned external fields is given as [41].

$$\mathcal{H} = -\frac{1}{2m^*}\left(\mathbf{P} + \frac{e}{c}\mathbf{A}(\mathbf{r})\right)^2 + \langle V_{ATDD}(z, \alpha_0)\rangle + eFz, \tag{1}$$

where m^* is the electron effective mass, $\mathbf{P}$ is the electron momentum operator, e is the electronic charge of the electron, c is the velocity of the light in the vacuum, $\mathbf{A}(\boldsymbol{r}) = (0, -Bz, 0)$ is the magnetic vector potential in the Landau gauge, z denotes the growth-direction of this structure, and $\langle V(z, \alpha_0)\rangle$ is the laser-dressed asymmetric triple delta-doped confining potential which is given by the following expression [42–44].

$$\langle V(z, \alpha_0)\rangle = \frac{\varpi}{2\pi}\int_0^{2\pi/\varpi} V(z + \alpha_0 \sin \varpi t)dt. \tag{2}$$

Here $\alpha_0 = eF_0/m^*\varpi$ is called the laser-dressing parameter, F_0 and ϖ are the strength and the non-resonant frequency of the laser field, and $V(z)$ is the confinement potential of the system in the absence of high-frequency ILF. It is worth commenting that the assumption of the laser-dressed model takes into account that the photon energy of the ILF is, actually, much larger than the energy distances of the subband's minimums in the considered system.

The analytical expression used in this work for the potential profile is written in the framework of the Thomas-Fermi approximation within the one-dimensional local density functional theory, as suggested by Ioriatti [45]. The Thomas-Fermi theory has proven to be highly successful in order to obtain the electronic structure in δ-doped systems [20,21]. This theory allows us to avoid a long and troublesome self-consistent calculation, having an excellent quantitative agreement with it instead. In this way, the potential profile associated with the n-type asymmetric triple δ-doped QW is given as

$$V(z) = -\frac{\eta^2}{(\eta\,|\,z - L_w/2\,| + z_{oL})^4} - \frac{\eta^2}{(\eta\,|\,z\,| + z_{oM})^4} - \frac{\eta^2}{(\eta\,|\,z - L_w/2\,| + z_{oR})^4}. \tag{3}$$

Here L_w is the effective width of the system. In the present work it essentially corresponds to the separation between the left and the right-hand side δ-doped QWs, $\eta = (e^2(2\ \mathrm{m}^*)^{3/2})/(15\pi\varepsilon\hbar^3)$, $z_{oL} = (2\varepsilon\eta^3/(\pi e^2 N_{2d}^L))^{1/5}$, $z_{oM} = (2\varepsilon\eta^3/(\pi e^2 N_{2d}^M))^{1/5}$, $z_{oR} = (2\varepsilon\eta^3/(\pi e^2 N_{2d}^R))^{1/5}$ are the local-density Thomas-Fermi parameters, ε is the static dielectric constant, N_{2d}^L, N_{2d}^M and N_{2d}^R label the density of donors in the left, central and right-hand side δ-doped layers, respectively.

To obtain solution of the eigensystem, $\mathcal{H}\phi = E\phi$, we have adopted the diagonalization method put forward by Xia & Fan [46]. According to this work, the single electron wave function $\phi(z)$ can be represented as the following expansion

$$\phi(z) = \left(\frac{2}{L_\infty}\right)^{1/2}\sum_{n=1}^{\infty} C_n sin\left(\frac{n\pi z}{L_\infty} + \frac{n\pi}{2}\right). \tag{4}$$

After detection the electron eigenfunctions and its corresponding eigenvalues, we can make use of the mathematical expressions for the total optical absorption coefficient and relative refractive index changes [38–41]. These are, respectively:

$$\beta^{(1)}(\omega) = \omega\sqrt{\frac{\mu}{\epsilon_r}}\frac{|M_{10}|^2\rho_{10}\hbar\Gamma_{10}}{(\delta\mathcal{E})^2 + (\hbar\Gamma_{10})^2}, \tag{5}$$

$$\frac{\Delta n^{(1)}(\omega)}{n_r} = \frac{\rho_{10}|M_{10}|^2}{2n_r^2\epsilon_0}\frac{\delta\mathcal{E}}{(\delta\mathcal{E})^2 + (\hbar\Gamma_{10})^2}, \tag{6}$$

and

$$\beta^{(3)}(\omega, I) = -2\omega\sqrt{\frac{\mu}{\epsilon_R}}\left(\frac{I}{\epsilon_0 n_r c}\right)\frac{|M_{10}|^4\rho_{10}\hbar\Gamma_{10}}{((\delta\mathcal{E})^2 + (\hbar\Gamma_{10})^2)^2} \times\left(1 - \frac{|\delta M|^2}{|2M_{10}|^2}\frac{(\delta\mathcal{E})^2 - (\hbar\Gamma_{10})^2 + 2\Delta E\delta\mathcal{E}}{(\Delta E)^2 + (\hbar\Gamma_{10})^2}\right) \tag{6a}$$

$$\frac{\Delta n^{(3)}(\omega, I)}{n_r} = -\frac{\mu c\,|M_{10}|^2}{4n_r^3\epsilon_0}\frac{\rho_{10} I}{((\delta\mathcal{E})^2 + (\hbar\Gamma_{10})^2)^2} \times\left[4(\delta\mathcal{E})\left|M_{10}\right|^2 - \frac{(\delta M)^2}{(\Delta E)^2 + (\hbar\Gamma_{10})^2}\{(\delta\mathcal{E}) \times((\Delta E)(\delta\mathcal{E}) - (\hbar\Gamma_{10})^2) - (\hbar\Gamma_{10})^2(2(\Delta E) - \hbar\omega)\}\right], \tag{7}$$

where $\delta M = M_{11} - M_{00}$ and $\delta\mathcal{E} = \Delta E - \hbar\omega$. The total optical absorption coefficient, $\beta(\omega, I)$, and the relative refractive index changes, $\Delta n(\omega, I)/n_r$, can be written as the sum of their linear and nonlinear components, respectively. In the expressions above, n_r is the refractive index of

the structure, μ is the magnetic permeability, ϵ_0 is the dielectric permittivity of the vacuum, ω is the angular frequency of the incident photon, I is the intensity of electromagnetic field, $\Delta E = E_1 - E_0$ is the energy difference between initial and final states, $M_{ij} = |<\psi_i|ez|\psi_j>|$ with $i, j = (0, 1)$ is the matrix element of the dipole operator for z-polarization of the light, $\Gamma_{10} = 1/\tau_{10}$ indicates the relaxation rate of the final and the initial states, and $\rho_{10} = m^*(E_1 - E_0)/(\pi\hbar^2 L_w)$ is the electron density in the QW.

3. Results and discussion

In this section, we present the numerical results of the effects of the static electric, the magnetic, and the high-frequency intense THz laser fields on the total optical absorption coefficient and the relative refractive index changes in the ATDD GaAs QWs. All calculations were performed using the following parameters: $m^* = 0.067m_0$ (where m_0 is the free electron mass), $\mu = 4\pi \times 10^{-7}\ Hm^{-1}$, $N_{2d}^L = 7.0 \times 10^{12} cm^{-2}$, $N_{2d}^M = 5.0 \times 10^{12} cm^{-2}$, $N_{2d}^R = 3.0 \times 10^{12} cm^{-2}$, $I = 0.05$ MWcm^{-2}, $n_r = 3.2$, and $L_W = 20$ nm, and $\tau_{10} = 0.14$ ps (where $\tau_{10} = 1/\Gamma_{10}$). Finally, let us to remark that the suitable convergence of the wave-function to investigated low-laying states appears for the truncation series at $N = 100$ with $L_\infty = 100$ nm. The numerical method has been implemented in software Mathematica [47].

The panels (a)–(c) of Fig. 1 show the effect of the static electric, the magnetic, and the high-frequency intense THz laser fields on the confinement potential profile and the probability density for the envelope wave-functions of the ground and first excited states in the n-type asymmetric triple δ-doped GaAs QWs. As it can be seen in the panel (a) of Fig. 1, the high-frequency THz laser field applied perpendicular to the growth-direction decreases the potential depth of the confinement potential of the system while decreasing the effective length of the confinement potential. With this effect of the laser field on the system, the triple QW structure transforms into a single QW structure and the energy difference between the subband energy levels of the structure increases. Frame (b) of Fig. 1 shows that due to the influence of the static electric field applied in parallel to the growth-direction of the structure, the confinement potential profile of the structure is bent and the energy interval between the ground and first excited states is increased. In addition, with the effect of the electric field on the structure, the system's ground state wave function is localized in the left QW of the structure. On the other hand, as it can be seen from panel (c) of Fig. 1, the magnetic field applied perpendicularly to the growth-direction of the system provides an additional geometric confinement to the system. The energy difference between the ground and first excited states increases due to the additional magnetic quantization. In addition, the influence of the magnetic field causes the probability density of ground state to localize at the central QW region. As a result, it can be noticed from these graphics that the applied external fields modify the potential confinement profile of the system in a significant way thus leading to changes in the intersubband transition energies and the wave-function distribution. These results clearly point at the tunability of the intersubband transitions in the conduction band of the structure induced by the applied external fields. This tunability makes the system a good candidate for new electronic and optoelectronic devices.

The changes of the energy interval between the lowest two confined energy levels and the off-diagonal dipole matrix elements between these energy states in the asymmetric triple δ-doped GaAs QWs, given as functions of (a) ILF parameter, (b) static electric field strength, and (c) the magnetic field induction are presented in panels (a)–(c) of Fig. 2. The red (blue) line in these figures represents the energy levels difference $E_1 - E_0$ (the variation of the dipole moment matrix elements (M_{10} and $M_{11} - M_{00}$). It is clearly noticed from all these three figures that the strengthening of the external fields leads to an increment of the intersubband energy difference, while the magnitude of the M_{10} dipole moment matrix element decreases in all cases. The magnitude of the $M_{11} - M_{00}$ dipole moment matrix element increases with the strengthening of the static electric and magnetic fields, while the increment of the THz laser field parameter α_0 causes it a decrease. These physical quantities are the main reasons for the increase (decrease) in the magnitude of the resonant peak of total optical absorption coefficient and the relative refractive index changes, and they shift the peak position, as it will be seen below.

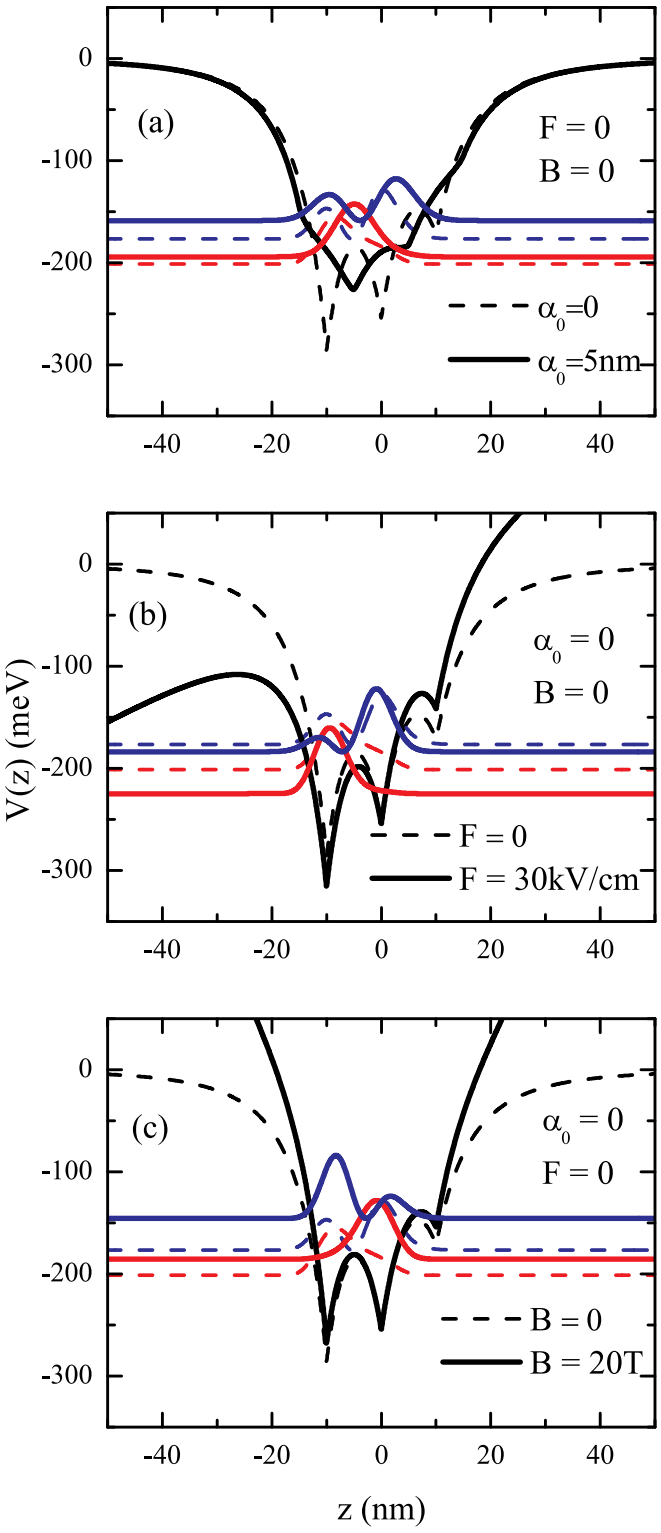


Fig. 1. Confinement potential and squared wave functions as a function of the growth direction for two different values of (a) the laser dressing parameter, (b) the static electric, and (c) the static magnetic field.

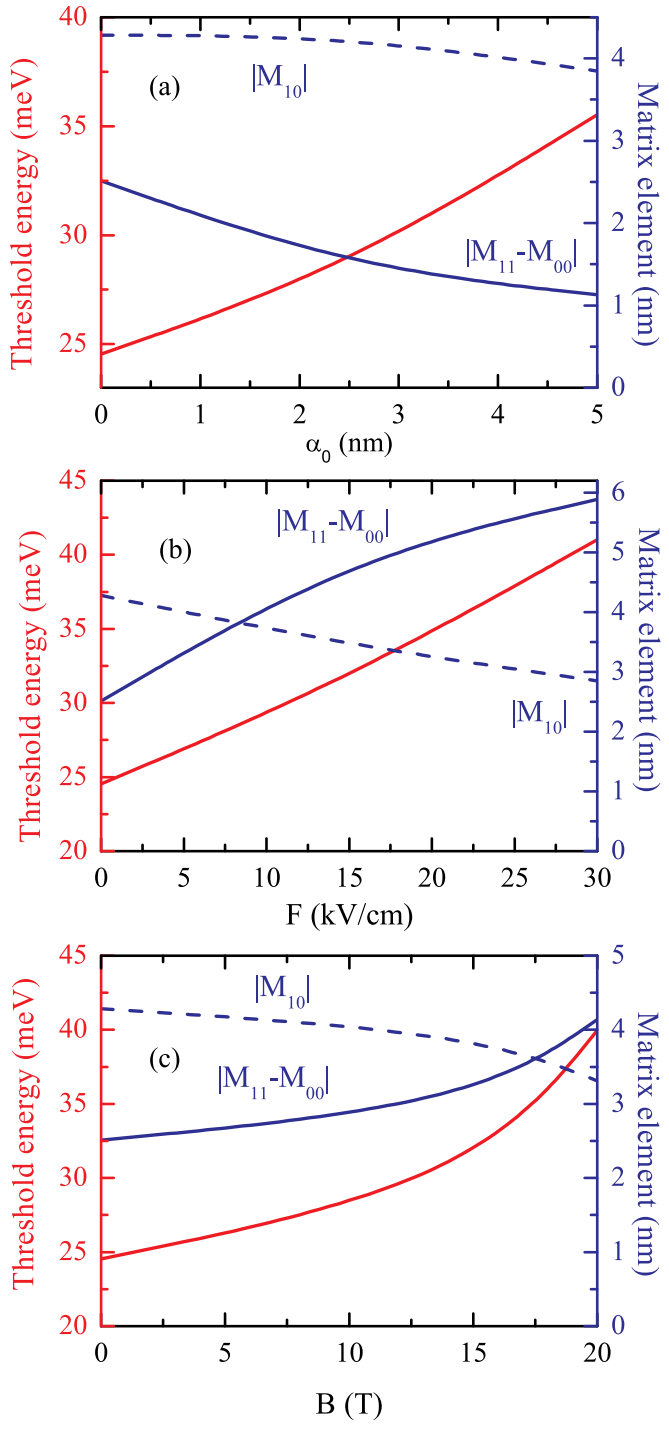


Fig. 2. Variations of the energy gap between the ground state and the first excited state and the matrix elements associated to the difference transitions between electron energy levels in the n-type triple δ-doped GaAs as a function of (a) the ILF parameter, (b) the electric field strength, and (c) the magnetic field induction.

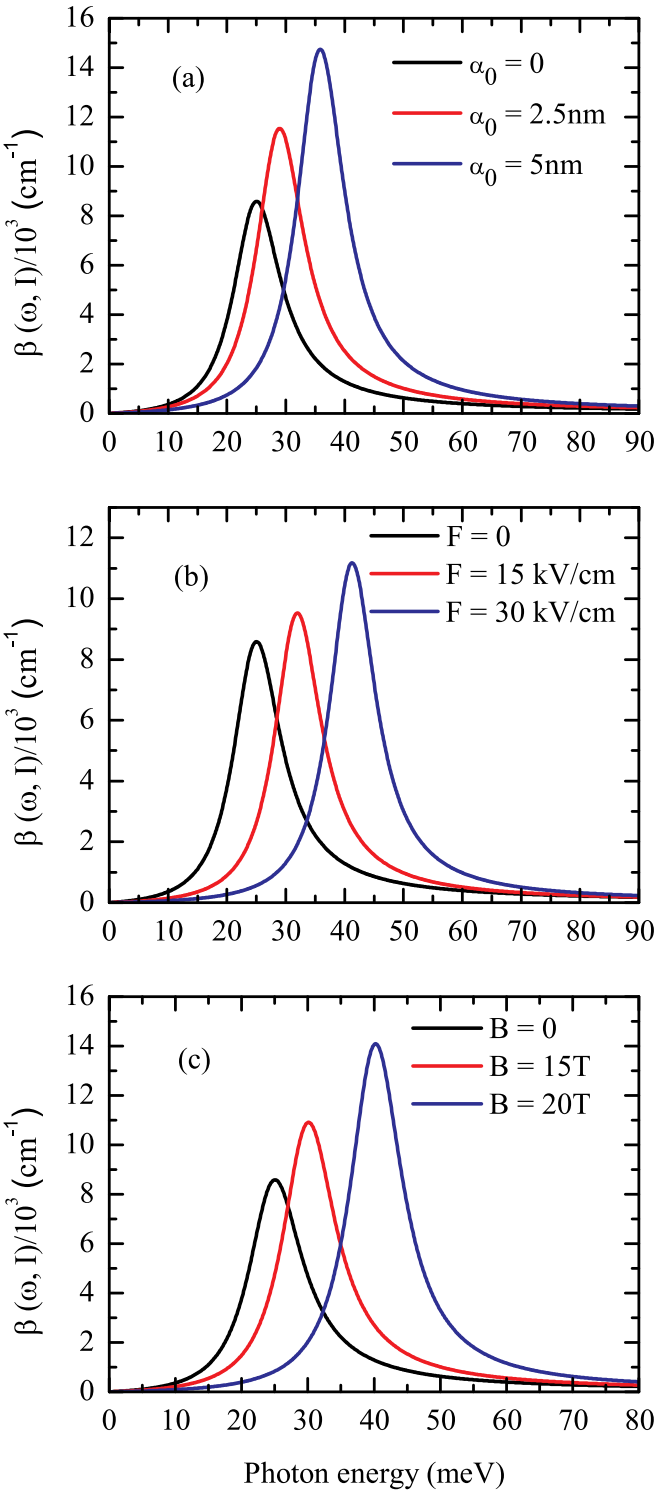


Fig. 3. Total optical absorption coefficient for intersubband transitions as a function of the incident photon energy for three different values of (a) the laser dressing parameter, (b) the static electric, and (c) the static magnetic field.

The panels (a)–(c) of Fig. 3 present the total optical absorption coefficient as a function of the incident photon energy for different values of the electric field strength, the magnetic field induction and the ILF parameter α_0. From these figures, it is clearly seen that similar to the changes of the energy difference between the ground and the first excited state with the corresponding magnitude of applied external fields, the total optical absorption coefficient shows a blue-shift as long as the magnitude of the external fields increases. This figure also shows that the maximum value of the total optical absorption coefficient increases with increase of the magnitude of the external field. This is explained by competition between the decrease of the dipole moment matrix element M_{10} value and the growth of the resonant frequency (the intersubband transition one), in which the latter element plays the leading role in all cases. Owing to these results, we can say that the magnitude of the applied external fields can be used as a tuning parameter to determine the position and magnitude of the peak value of the total optical

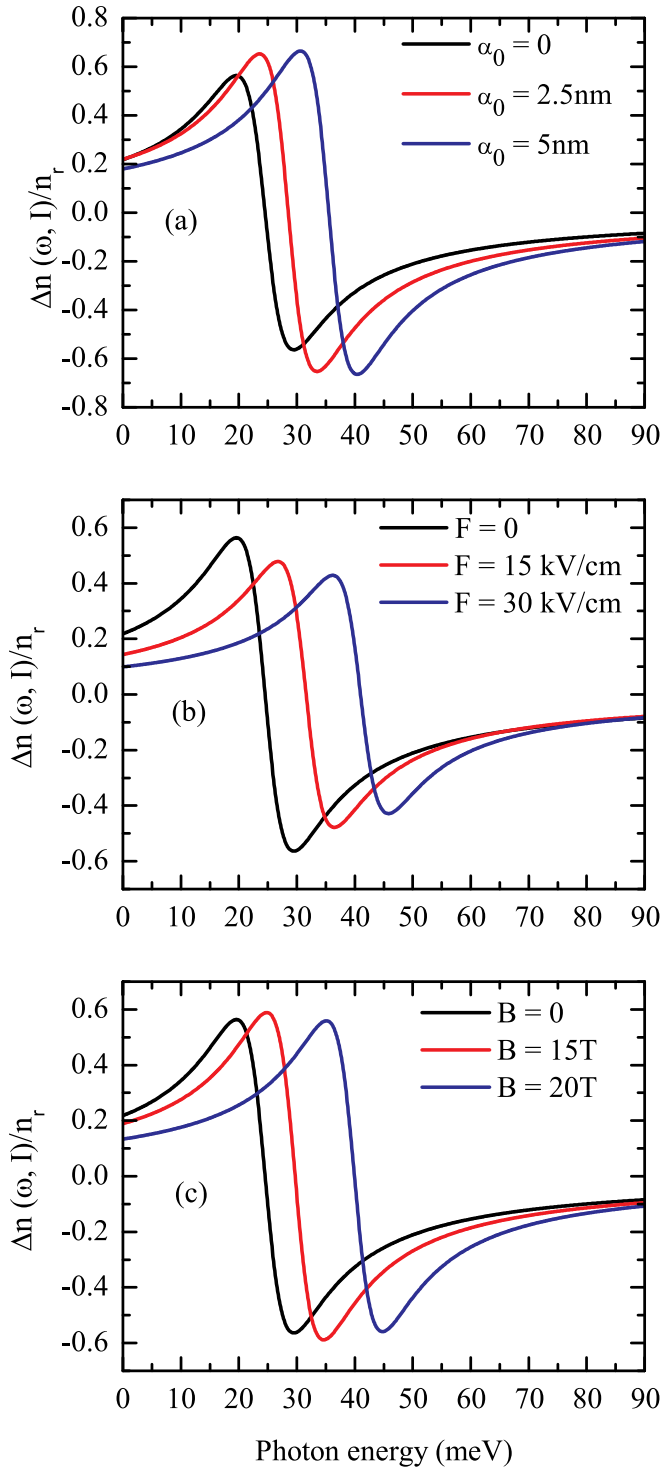


Fig. 4. Relative refractive index changes for intersubband transitions as a function of the incident photon energy for three different values of (a) the ILF parameter, (b) the static electric strength, and (c) the magnetic field induction.

absorption coefficient. A similar situation is treated in Refs. [48,49]. The authors of Ref. [48] calculated the subband structure of triple δ-doped GaAs structure by using the self-consistently Schrödinger and Poisson equations. Also, the author of [49] investigated the total optical absorption coefficients and the relative refractive index changes in single, double, and triple δ-doped GaAs structures. The authors obtained the same type of behavior for triple δ-doped GaAs structure.

The panels (a)–(c) of Fig. 4 show the relative refractive index changes related to the structure against the incident photon energy. In this case, we depict the relative refractive index changes for three different of ILF parameter (0, 25 and 100 $\AA$), for three different values of static electric field strength (0, 15, and 30 kV/cm), and for three different values of magnetic field induction (0, 15, and 20 T). In Fig. 4(a) and (c) can be observed that as the magnitude of ILF parameter α_0 and magnetic field induction B are increased, the amplitude of the relative refractive index changes is also increased. This is due to the dipole moment matrix element M_{10} in Eq. (5) and its change according to the laser field and the magnetic field provided. Frames (a) and (c) of Fig. 2 show that as the laser field and the static magnetic field increase, M_{10} decreases. Moreover, it can be seen that with the increment of the ILF parameter and the magnetic field induction, the resonant peaks of the relative refractive index changes shift to a high energy region (blue shift). It is easily seen from the panel (b) of Fig. 4 that when the static electric strength field increases, the resonant peak of the relative refractive index changes decreases and it shifts to a high energy region. In order to interpret these properties, the subband energy differences and the dipole moment matrix elements are shown in the panel (b) of Fig. 2. Besides, the amplitude of the relative refractive index changes decreases by the growth of the $M_{11} - M_{00}$ values when the static electric strength field is also increased.

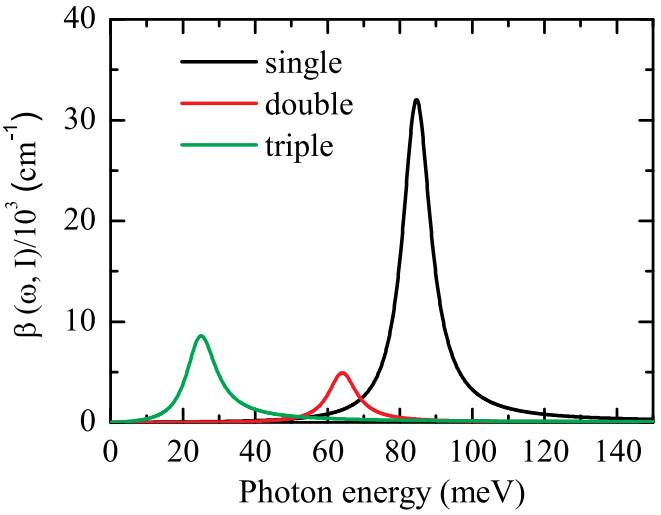


Fig. 5. Total optical absorption coefficient for intersubband transitions as a function of the incident photon energy for three different number of the QW in the absent of external fields ($\alpha_0 = 0$, $F = 0$, $B = 0$).

Finally, Fig. 5 represents the total optical absorption coefficient as a function of incident photon energy in the absence of external fields ($\alpha_0 = 0$, $F = 0$, $B = 0$). For all cases, the effective width $L_w = 20$ nm is kept constant. The green line corresponds to the total absorption coefficient of triple QWs. The red line corresponds to the case of double QWs for the following values of parameters $N_{2d}^L = 7.0 \times 10^{12} cm^{-2}$, $N_{2d}^M = 0$, $N_{2d}^R = 3.0 \times 10^{12} cm^{-2}$. And finally, the black line corresponds to case of single QW when $N_{2d}^L = 7.0 \times 10^{12} cm^{-2}$, $N_{2d}^M = 0$, $N_{2d}^R = 0$. As it can be is seen from the figure with the decrease of the number of QW, the total absorption coefficient maximum shifts to the high photon energy region (blue shift). With a decrease in the number of QW, the electron localization effective length for low-lying states decrease, which leads to the increment of energy levels. Due to this, the threshold energy of the corresponding state increase and the blue shift in the total optical absorption spectrum is observed.

4. Final remarks

In the present work, we have theoretically studied the simultaneous effect of the static electric and the magnetic fields, as well as the intense THz laser field on the intersubband optical properties of the asymmetric triple δ-doped GaAs QWs, such as the total optical absorption

coefficient and the relative refractive index changes. The subband energy levels and related envelope wave functions have been calculated solving the Schrödinger equation within the framework of the high-frequency Floquet theory by using the exact diagonalization technique. The total optical absorption coefficient and relative refractive index changes have been inferred from the compact-density matrix approximation. The obtained results reveal that the threshold energies of intersubband transitions, total optical absorption coefficient, and the relative refractive index changes are significantly affected by the external fields. Thus, the total absorption coefficient and the relative refractive index changes with certain desired values can be obtained by using a properly adjusted external field strength. Furthermore, we believe that, by considering the effect of the external field and the asymmetry of the n-type asymmetric triple δ-doped GaAs QWs, it is possible to adjust the optimum optical response of the optoelectronic devices based on these structures.

Acknowledgments

MGB acknowledges the financial support by the Armenian State Committee of Science (Project no. 18T-1C223). DL and LMP acknowledge partial financial support from FONDECYT 1180905. DL acknowledges partial financial support from Centers of excellence with BASAL/CONICYT financing, Grant FB0807, CEDENNA.

References

[1] T. Kobayashi, T. Ariki, M. Iwabuchi, T. Maki, S. Shikama, S. Suzuki, J. Appl. Phys. 76 (1994) 1977.
[2] L.M.R. Scolfaro, D. Beliaev, J.R. leite, A.T. Lino, E.K. Takahashi, Int. J. Quantum Chem. 28 (1994) 667.
[3] Y. Anda, T. Ariki, T. Kobayashi, Jpn. J. Appl. Phys. 34 (1995) 3987.
[4] C. Tolksdorf, J. Schulze, T. Sulima, I. Eisele, G. Deboy, 60th DRC Conference Digest Device Research Conference (Proc.), (2002), pp. 85–86.
[5] A. Denisenko, E. Kohn, Diam. Relat. Mater. 14 (2005) 491.
[6] H.-Y. Chang, E.-K. Lee, B.V. Kamanev, J.-M. Baribeau, D.J. Lockwood, L. Tsybeskov, Mater. Res. Soc. Symp. Proc. 958 (2007) 0958-L10-23.
[7] H. El-Hajj, A. Denisenko, A. Bergmaier, G. Dollinger, M. Kubovic, E. Kohn, Diam. Relat. Mater. 17 (2008) 409.
[8] H.E.- Hajj, A. Denisenko, A. Kaiser, R.S. Balmer, E. Kohn, Diam. Relat. Mater. 17 (2008) 1259.
[9] H. El-Hajj, Growth and Characterization of Diamond δ-Doped Layers for FET Applications, Ph. D. Thesis (University of Ulm, 2009.
[10] N. Tumilty, J. Welch, H. Ye, R.S. Balmer, C. Wort, R. Lang, R.B. Jackman, Appl. Phys. Lett. 94 (2009) 052107.
[11] H. Yin, P. Ziemann, Appl. Phys. Lett. 104 (2014) 252111.
[12] J.H. Park, S. Ozaki, N. Mori, C. Hamaguchi, Superlattice Microstruct. 25 (1999) 445.
[13] E.F. Schubert, K. Ploog, Jpn. J. Appl. Phys. 24 (1985) L608.
[14] G. Abstreiter, R. Merlin, A. Pinczuk, IEEE J. Quantum Electon. 22 (1986) 1771.
[15] A. Zrenner, et al., Semicond. Sci. Technol. 3 (1988) 1203.
[16] M. Santos, et al., Mater. Sci. Eng. B 53 (1988) 2504.
[17] F. Koch, A. Zrenner, Mater. Sci. Eng. B 1 (1989) 221.
[18] N. Schwarz, et al., Semicond. Sci. Technol. 4 (1989) 571.
[19] J. Wagner, A. Fischer, K. Ploog, Phys. Rev. B 42 (1990) R7280.
[20] L.M. Gaggero-Sager, R. Pérez-Alvarez, J. Appl. Phys. 78 (1995) 4566.
[21] L.M. Gaggero-Sager, Model. Simul. Mater. Sci. Eng. 9 (2001) 1.
[22] C.R. Lu, S.K. Du, J.R. Anderson, D.R. Stone, R.A. Wilson, Appl. Surf. Sci. 92 (1996) 543.
[23] C. Jagadish, G. Li, M.B. Jonston, M. Gal, Mater. Sci. Eng. B 51 (1998) 103.
[24] E. Ozturk, Y. Ergun, H. Sari, I. Sökmen, J. Appl. Phys. 91 (2002) 2118.
[25] J.C. Martínez-Orozco, L.M. Gaggero-Sager, S.J. Vlaev, Soli-State Elect. 48 (2004) 2277.
[26] I. Rodríguez-Vargas, L.M. Gaggero-Sager, J. Appl. Phys. 99 (2006) 033702.
[27] R.L. Restrepo, M.G. Barseghyan, M.E. Mora-Ramos, C.A. Duque, Physica E 51 (2013) 48.
[28] E. Ozturk, Y. Ozdemir, Opt. Commun. 294 (2013) 361.
[29] K.A. Rodríguez-Magdaleno, J.C. Martínez-Orozco, I. Rodríguez-Vargas, M.E. Mora-Ramos, C.A. Duque, J. Lumin. 147 (2014) 77.
[30] H. Dakhlaoui, Superlattice Microstruct. 97 (2016) 439.
[31] J.C. Martínez-Orozco, J.G. Rojas-Briseño, K.A. Rodríguez-Magdaleno, I. Rodríguez-Vargas, M.E. Mora-Ramos, R.L. Restrepo, F. Ungan, E. Kasapoglu, C.A. Duque, Physica B 525 (2017) 30.
[32] T.W. Kim, Y. Kim, S.K. Min, Thin Solids Fims 254 (1995) 61.
[33] R. Sasagawa, H. Sugawara, Y. Ohno, H. Nakajima, S. Tsujino, H. Akiyama, H. Sakaki, Appl. Phys. Lett. 72 (1998) 719.
[34] H. Yildirim, M. Tomak, Phys. Status Solidi(b) 12 (2006) 2874.
[35] J.C. Martínez-Orozco, M.E. Mora-Ramos, C.A. Duque, J. Lumin. 132 (2012) 449.
[36] S. Almansour, H. Dakhlaoui, E. Algrafy, Chin. Phys. Lett. 33 (2016) 027301.
[37] H. Sari, U. Yesilgul, F. Ungan, S. Sakiroglu, E. Kasapoglu, I. Sökmen, Chem. Phys. 487 (2017) 11.
[38] V.N. Mughnetsyan, A.Kh Manaselyan, M.G. Barseghyan, A.A. Kirakosyan, J. Lumin. 134 (2013) 24.
[39] E. Kasapoglu, U. Yesilgul, F. Ungan, I. Sökmen, H. Sari, Opt. Mater. 64 (2017) 82.
[40] F. Ungan, M.E. Mora-Ramos, E. Kasapoglu, H. Sari, I. Sökmen, Optik 180 (2019) 387.
[41] H. Sari, F. Ungan, S. Sakiroglu, U. Yesilgul, I. Sökmen, Optik 162 (2018) 76.
[42] F.M.S. Lima, M.A. Amato, O.A.C. Nunes, A.L.A. Fonseca, B.G. Enders, E.F. da Silva Jr., J. Appl. Phys. 105 (2009) 123111.
[43] A. Radu, A.A. Kirakosyan, D. Laroze, H.M. Baghramyan, M.G. Barseghyan, J. Appl. Phys. 116 (2014) 093101.
[44] H.M. Baghramyan, M.G. Barseghyan, A.A. Kirakosyan, J.H. Ojeda, J. Bragard, D. Laroze, Sci. Rep. 8 (2018) 6145.
[45] L. Ioriatti, Phys. Rev. B 41 (1990) 8340.
[46] J.-B. Xia, W.-J. Fan, Phys. Rev. B 40 (1989) 8508.
[47] Wolfram Mathematica Version 11, USA.
[48] E. Ozturk, H. Sari, Y. Ergun, I. Sökmen, Appl. Phys. A 80 (2005) 167–171.
[49] E. Ozturk, Rom. J. Phys. 602 (2017) 603–610.